Correspondence to:
M. M. F. Saba,
marcelo.saba@inpe.br

High-Speed Video Observation of a Dart Leader Producing X-rays

M. M. F. Saba[1] , M. A. S. Ferro[2] , E. T. Cuadros[1], D. M. Custódio[2] , A. Nag[3] ,
C. Schumann[4] , V. Cooray[5], A. R. Paiva[1], P. B. Lauria[1], D. S. F. Medeiros[1],
P. Hettiarachchi[5] , and H. K. Rassoul[3]

[1]National Institute for Space Research, São José dos Campos, Brazil, [2]Institute of Aeronautics and Space, São José dos Campos, Brazil, [3]Florida Institute of Technology, Melbourne, FL, USA, [4]School of Geosciences, University of Witwatersrand, Johannesburg, South Africa, [5]Department of Engineering Sciences, Uppsala University, Uppsala, Sweden

Abstract This work presents the first simultaneous X-ray measurement and high-speed video observation of the propagation of a lightning leader producing X-rays. As a result, the three-dimensional leader distance from the X-ray measurement and, for the first time, the conditions of the preexisting channel during the leader propagation were observed. Although four leaders in this seven-stroke flash followed the same path to ground, X-rays were only observed during the leader before the return stroke with the highest peak current. The fact that the other three leaders following the same path to ground did not produce detectable X-rays confirms the hypothesis that leader line charge density is an important factor that determines X-ray production. The fact that X-rays was recorded only when the leader tip was at a certain portion of the lightning channel confirms that the orientation of the leader plays an important role in the detection of X-rays.

Plain Language Summary It was known that lightning can produce X-rays. However, in this study, thanks to the use of a high-speed video camera it was possible to determine when lightning produces X-rays, how far it was, how it was oriented when the detection of X-rays, and what the conditions of the preexisting channel were during the leader propagation. The observations of the present work allow for new insights, confirmation of some hypotheses, and comparison with past studies. The results presented help to understand why X-rays are sometimes detected and sometimes not. It is shown that the amount of charge transferred by the discharge plays a crucial role. This study also confirms that the orientation of the descending leader plays an important role in the detection of X-rays.

1. Introduction

Lightning emits X-rays. Although progress has been achieved in quantifying some properties of the lightning-leader X-ray emission in natural, rocket-triggered, and upward lightning (e.g., Moore et al., 2001, Dwyer et al., 2003, Dwyer et al., 2004, Dwyer et al., 2005, Dwyer et al., 2011; Saleh et al., 2009; Yoshida et al., 2008; Howard et al., 2008, Howard et al., 2010; Mallick et al., 2012; Hettiarachchi et al., 2018), it is still uncertain why not all strokes in the same flash and not all leader steps in the same stroke produce detectable X-rays.

Howard et al. (2010) reported observations of leader electric fields and generation of energetic radiation close to triggered lightning. The authors suggest that the X-ray emissions may be beamed to some degree in the direction of the leader propagation. Saleh et al. (2009) however found that their observations were most consistent with an isotropic radiation source, although they could not rule out the possibility that the emissions become slightly beamed as the leader approaches very near the ground. More recently, Dwyer et al. (2011) and Schaal et al. (2014) used a pinhole-type X-ray imaging camera in order to produce two-dimensional "photos" and "movies" of the X-ray source regions of dart leaders in triggered lightning. They found that the X-ray source is located near and descends with the leader front and that two distinct X-ray emission patterns (compact and diffuse) may be present in lightning leaders.

Montanya et al. (2012) attribute the difficulty of measuring X-rays to some beaming of the high-energy particles from the leader and to the requirement that the detectors must be close enough in order not to receive completely attenuated radiation. This may explain why the catalogue of X-ray measurements produced by

natural lightning is very small (Moore et al., 2001; Dwyer et al., 2005a; Howard et al., 2008; Howard et al., 2010; Mallick et al., 2012; Montanyà et al., 2012; Schaal et al., 2012). All these observations, except those of Mallick et al. (2012), correspond to stepped leaders, not natural dart leaders.

Furthermore, a theoretical work conducted by Cooray et al. (2010) states that charge that exists at the tip of the dart leader is responsible for driving the electrons to runaway energies, resulting in X-ray emissions. Therefore, some dart leaders may not produce X-rays at all or at least not at a detectable level.

In order to understand the mechanisms producing the X-rays and the source regions of the emissions, simultaneous recording of high-speed video of the leader together with X-ray measurements have been tried in past studies but has not been successful (e.g., Montanyà et al., 2012; Montanyà et al., 2014; Schaal et al., 2012).

This work presents the measurements of X-rays from a natural lightning dart leader. Moreover, it presents the first high-speed video observation of a leader producing X-rays during its propagation to ground. The high-speed video images in conjunction with other measurements not only made it possible to address some factors considered important in theoretical studies but also factors that affected the observation of X-rays in all previous studies such as distance, leader charge, trajectory, and channel temperature.

In contrast with previous studies, video images from different angles allowed us to calculate the three-dimensional distance from the X-ray detector and the orientation of the channel when the X-ray detector observed radiation from the leader. It also made possible to check the status of the lightning channel by knowing how many strokes and continuing current events had previously conditioned the channel. It was also possible to compare the luminosity of the dart leader producing X-rays with the other ones that did not produce any detectable radiation. The use of a fast electric-field sensor together with the estimated peak current of the prospective return stroke made possible to qualitatively estimate the charge involved in each dart leader. The reported observations have important implications for understanding why some leaders produce detectable energetic radiation and some leaders not.

2. Instrumentation

The X-ray detection system was installed inside an aluminum box of thickness 3.1 mm on the top of 50-m-tall building located in the city of São Paulo (785 m above sea level), Brazil. The detecting system was composed by a 7.6×7.6-cm cylindrical NaI (Tl)/Photomultiplier tube (PMT) which contained internal HV supplies and divider chains. The detector used is identical to the detector described in more detail in the papers of Saleh et al. (2009). However, as a preamplified output coming from the PMT was used instead of the direct anode output (see Saleh et al., 2009; Figure 2), the X-ray detecting system had a slower response due to the higher decay constant of the preamplifier. A fiber-optic link (a DG Instruments FOS1 with a bandwidth of 5 MHz, and input voltage ± 1 V) carried the detector signal through a 120-m-long fiber optic to a data logger recording at a sampling rate of 5 MS/s. The X-ray detection system (the detector and fiber-optic transmitter) was powered by two 12-V batteries also housed inside the same aluminum box and replaced by charged ones when necessary. This arrangement guaranteed very good noise immunity.

The 5-MS/s sample rate data logger was also utilized to record the vertical electric-field measurements. In order to have time synchronization in all measurements a GPS receiver is connected to the data logger (a PC with a GPS card Meinberg GPS170PCI and a 12-bit data acquisition card NI PCI-6110).

The electric field sensor consisted of a flat plate antenna with an integrator and amplifier. It was also located at the top of the building, 3 m away from the X-ray system. A fiber-optic link was also used to transmit the signal from the integrator/amplifier to the digitizer. The bandwidth of the system ranged from 306 Hz to 1.5 MHz. The physics sign convention will be used when referring to the electric field and its change. The approach of a nearby negative leader produces positive electric field change and a negative CG return stroke produces a negative field change.

In addition to the X-rays and vertical electric field sensors, a high-speed camera and two standard speed cameras were also used. The high-speed camera used was a Phantom V711 operating at 37,819 frames per second with time interval between frames of 26.44 μs and exposure time of 26.08 μs (at the end of each frame the camera is blind for 0.36 μs due to data transfer). Each frame of the video is time stamped by means of a
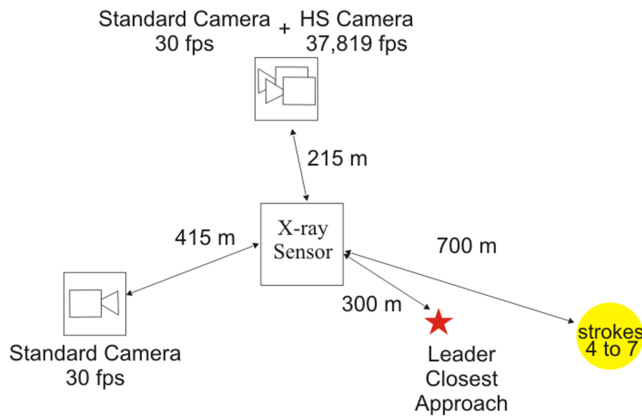
Figure 1. X-ray measurement system and the distances from cameras, from ground contact strike point of strokes 4 to 7, and from the closest segment of the lightning stroke that produced X-ray radiation. All distances are ground projection distances, except the leader closest approach distance, which is a 3-D distance.

GPS antenna. The Phantom V711 and a standard video camera (30 frames per second) were installed at a distance of 220 m from the X-ray sensor. The other standard camera was at 415 m from the X-ray sensor but at an angle of 108° with the high-speed camera (Figure 1).

Information obtained from two lightning location systems was used to estimate the location and the peak current of the return strokes. More details about these lightning location systems and their performances can be found in Naccarato and Pinto (2009) and Saba et al. (2017).

3. Data Presentation

On 16 December 2018 (18:43:37 UT) a seven stroke downward negative cloud-to-ground flash followed by a very long continuing current (lasting 630 ms) struck the ground close to the X-ray system. Some characteristics of the strokes are documented in Table 1.

The first three strokes of the seven-stroke flash followed different paths to ground. The second and the third strokes were completely out of the field of view of the cameras. The fourth leader after following the initial portion of the first return stroke channel, initiated a new path to ground and branched during its propagation. The subsequent stroke leaders used the same path to ground as the leader of the fourth return stroke but without branching and with a much higher speed. The average 2-D speed of the fourth leader and the relative average speed of subsequent leaders across the path observed by the high-speed camera are also indicated in Table 1. The X-ray detection occurred before the fifth return stroke (shown in bold numbers in Table 1) during the dart leader propagation. Upon inspecting the E field data during the leader propagation, we could not see a clear indication of discrete microsecond-scale electric field pulses that accompany leader steps in a dart-stepped leader. It seems that the fifth stroke may have been preceded by what is sometimes called a "chaotic leader" (as indicated in the paper of Stolzenburg et al. (2014)), although there is no branching during the occurrence of the dart leader and therefore it is not conclusive that it is a "chaotic leader."

Two lightning detection networks detected this flash. One of them (BrasilDAT) indicated the estimated peak current of each of the seven strokes. The other network (RINDAT) estimated the peak current of the first, second, and fifth strokes (indicated in brackets in Table 1). The reported peak current values by both lightning detection networks were almost identical. Based on the reported data given by the lightning detection networks and on the analysis of the images, the dart leader producing X-rays struck the ground at a distance of approximately 700 m from the X-rays detecting system (Figure 1).

Figures 2a and 2b show sequences of images of the leader propagation before the occurrence of return stroke 4 (RS 4) and return stroke 5 (RS 5), respectively. The electric field changes caused by the leaders are shown in

Table 1
Characteristics of the Return Strokes of the Negative Cloud-To-Ground Flash

| Return stroke	1	2	3	4	**5**	6	7
Time of each return stroke (UT)	18:43:37 458.725	490.040	550.482	601.615	**718.067**	770.178	818.985
X-ray detection	No	No	No	No	**Yes**	No	No
Continuing current duration (ms)	8	-	-	20	**17**	35	630
Time elapsed from previous stroke (ms)	-	31	60	51	**116**	52	49
Estimated peak current (kA)	−19 (−18)	−18 (−17)	−12	−6	**−38** (**−38**)	−6	−12
Leader positive field change (relative units)	498	820	88	859	**3398**	810	1064
Ground contact point	1	2	3	4	**4**	4	4
Propagation time of the leader along the visible portion of the channel (ms)	-	-	-	7.48	**0.27**	0.53	0.15
Relative speed (V_n/V_4) (V_4 is the average 2-D speed of leader preceding the fourth stroke = 49.2×10^3 m/s)	-	-	-	1.0	**28.1**	14.2	49.2
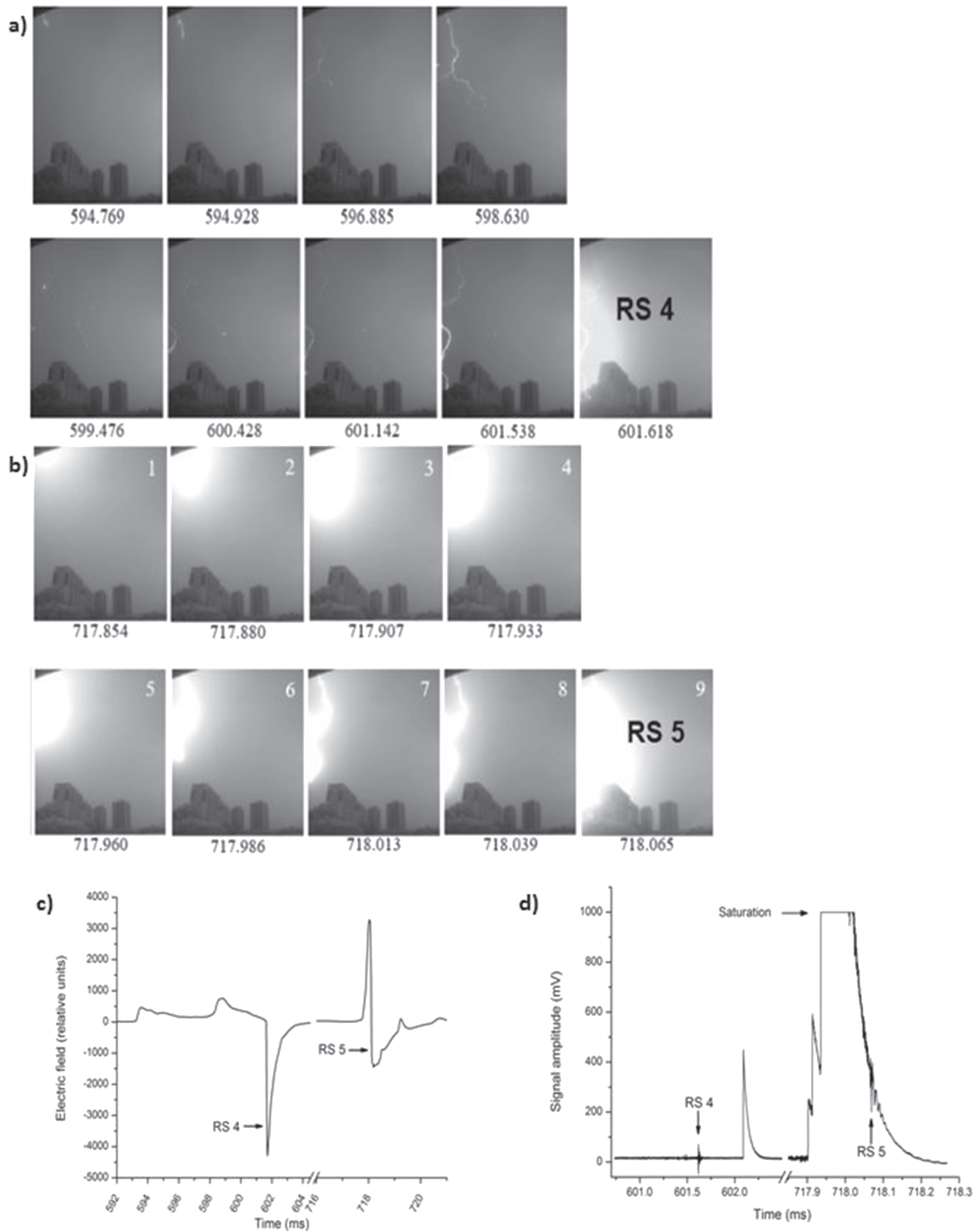
Figure 2. (a and b) Sequence of images of the leader propagation that preceded return strokes 4 and 5 and (c and d) the electric field changes and X-ray measurements before and after the return strokes. The numbers below the video images indicate the time of each frame in milliseconds at the end of the frame integration. The occurrence of the return strokes 4 and 5 and the saturation of the X-ray measurement are indicated by arrows in the plots.
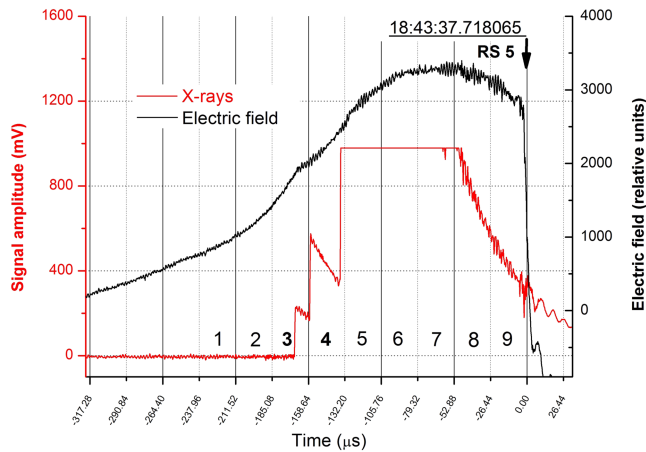
Figure 3. Electric field and X-ray measurements during the approach of the dart leader of RS 5.

Figure 2c. Both abrupt negative field changes caused by return strokes RS 4 and RS 5 are preceded by positive field changes. A long duration and small positive change due to the approach of a stepped leader precedes RS 4 and a short but intense positive change due to the dart leader precedes RS 5. The differences between the luminosity of each leader and the electric field change caused by each leader are patent. The X-ray measurements are shown in Figure 2d. Note the complete absence of X-ray detection during the leader propagation before return stroke 4. Similarly, no X-rays were detected during the propagation of the leaders that caused the other return strokes, except for stroke 5. The pulse occurring at approximately 0.5 ms after return stroke 4 in Figure 2d is a pulse of background radiation. The record of this pulse was included in the plot to illustrate how different it is from the radiation that is produced by the leader before return stroke 5. The pulses that appear at the moment of the return stroke 4 and 5, and indicated by arrows in the X-ray plot (Figure 2d), are due to the interference caused by these strokes in the data acquisition system.

In Figure 3 X-rays and the electric-field measurements are shown for the return stroke 5. The time interval between labels in the *x* axis (26.44 μs) of the graph corresponds to the time duration of each frame of the high-speed camera. Numbers 1 to 9 in the graph correspond to the nine high-speed video frames recorded during the propagation of the dart leader (shown in Figure 2). The integration of the image in frame number 9 in Figure 2 ends when the luminosity of the return stroke was already present, but not at its maximum value. Considering that (according to the lightning location system) the peak current of the return stroke occurred at 18:43:37.718067 and that the estimated zero-to-peak time was 3.7 μs, the return stroke may have started 2 or 3 ms before the end of the integration of frame 9 at 18:43:37.718065 (Figure 3).

One can observe in Figure 3 that three X-ray pulses were observed during intervals 3 and 4 (marked in bold numbers). The X-ray pulse at the end of frame interval 4 was very intense and saturated the measurement.

Figure 4 shows images of the lightning channel used by the last four strokes from two almost orthogonal standard video cameras. The numbered marks on the images show where the leader tip was at the end of the numbered intervals in Figure 3. Combining the video images of the high-speed camera and of the two almost orthogonal standard cameras it is possible to define with good approximation where the tip of the dart leader was during the detection of the X-rays.

4. Discussion

The high-speed video images showed that the first three strokes of the seven-stroke flash followed different paths to ground. All these different paths were at a greater distance from the X-ray detector than the path followed by the four last strokes. The fourth leader after following the same path as the first leader up to point indicated by the green arrow in Figure 4a, deviated from it through a new path and branched during its propagation to ground. The leader in this new path made a curve towards the X-ray detector and then away from it (Figure 4b). The following three dart leaders did not branch and followed the same path to ground as the fourth return stroke.

In previous theoretical and observational studies some features have been suggested as important factors that enable the detection of X-rays from lightning. Using the concurrent information from the high-speed images, electric-field sensor, X-ray sensor, and auxiliary cameras, four of them will be discussed: distance, leader charge, trajectory, and channel temperature.

If the X-ray source is far away from the sensor, air will attenuate the radiation and prevent any detection. This could be one of the reasons for the absence of any detection during the occurrence of the first three strokes. However, as all last four leaders followed the same path and only one of them produced detectable X-rays, trajectory, tortuosity, and distance from the sensor are not influencing the detection.
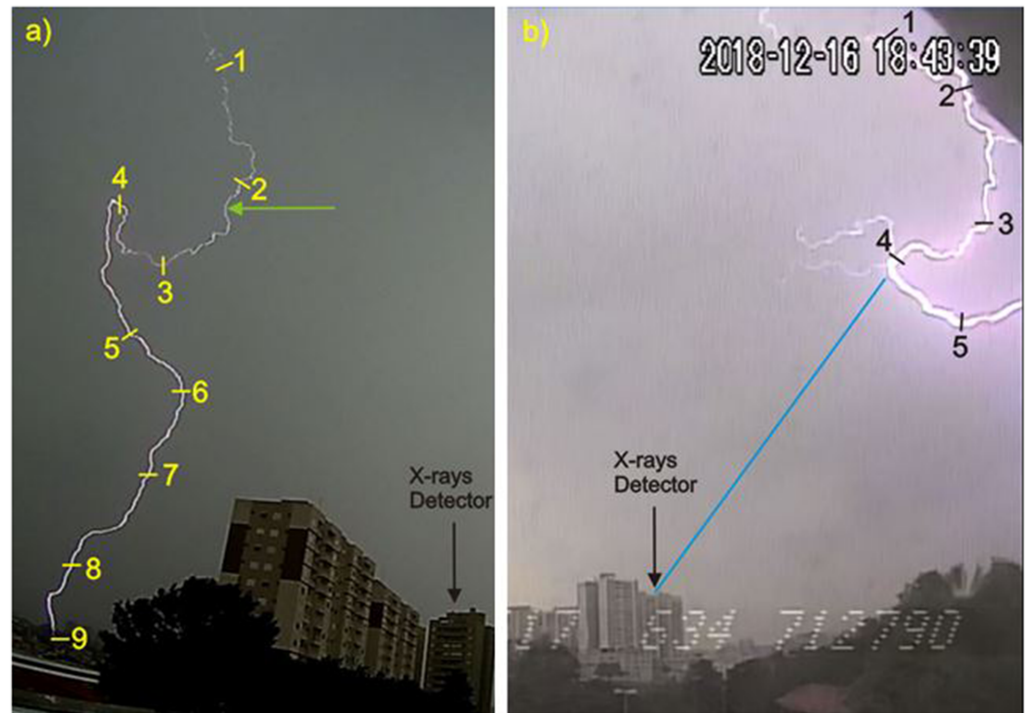
Figure 4. Images from two almost orthogonal standard video cameras. The numbered marks indicate the approximate location of the dart leader tip at the end of each video frames recorded by the high-speed camera during the fifth return stroke.

What is significantly different in the characteristics of the leader that produced X-rays is the luminosity (see Figure 2), the amplitude of the positive field change produced during the approach of the leader, and the estimated peak current of the prospective return stroke (Table 1). All these three characteristics are well associated. The return stroke peak current depends on the line charge density of the descending leader (Kodali et al., 2005), and the higher the charge is, the higher will be the current and the brighter will be the leader in the images. Therefore, high peak current return strokes are produced by highly charged and luminous leaders. We conclude that only the highly charged leader produced an electric field intense enough to produce detectable X-rays. This is an experimental confirmation, for natural lightning, of the theoretical prediction of Cooray et al. (2010) that the electric field at the tip of dart leaders is capable of producing high-energy radiation. An experimental evidence of this relationship had been previously reported by Schaal et al. (2012) for triggered lightning.

The analysis of the images also shows that during the descent of the leader of the fifth return stroke, the detection of the X-rays occurred only when the leader was at the closest distance from the detector (estimated three-dimensional distance of 300 ± 20 m). However, the leader was not only at the closest distance, but perhaps at such a position/orientation that the detector was within the X-ray flux beam as discussed by Howard et al. (2010) and Montanyà et al. (2014). Note that the most intense pulse of radiation (Figure 3) occurred when the leader was around mark 4 in Figure 4. The blue line drawn over Figure 4b connects this mark to the location of the detector on top of the building and suggests that the leader may have had been oriented towards the X-ray sensor when travelling around mark 4. Also, the abrupt rise of the X-ray intensity suggests that it was the orientation of the leader and not its distance that modulated the detected signal.

Finally, according to calculations performed by Cooray et al. (2010), the density of the defunct return stroke channel decreases with increasing temperature, and therefore, in a given dart leader electric field, the possibility of accelerating electrons to runaway mode increases with increasing temperature. They suggest that if it is higher than about 2,500 K, a typical dart leader with prospective return stroke current of 12 kA could accelerate electrons into energies in the range of MeV. Considering the long interstroke time interval (116 ms) preceding the fifth stroke, a low temperature in the defunct channel would be expected (even if

the 20-ms duration continuing current following the previous return stroke is considered; see Table 1). However, their model also predicts that this critical temperature (of 2,500 K) decreases with the increase in dart leader current (the peak of the prospective return stroke current). This may also be the case here. Therefore, our observations and measurements show that not only their hypothesis are confirmed but that the long interstroke interval, and therefore the lower channel temperature, is compensated by a relatively large leader current (as indicated by its luminosity), electric field change, and the peak current of the following return stroke (38 kA).

In conclusion, based on the simultaneous recording of high-speed video images, X-ray, and electric-field measurements we show that (a) for dart leaders following the same trajectory equally distant from the X-ray detector, only the highly charged leader will produce detectable X-rays; (b) although the leader was highly luminous (and therefore highly charged) throughout the trajectory, X-rays were recorded only when the leader tip was located at a certain portion of the lightning channel; (c) detection occurs when the leader is probably oriented toward the detector, supporting the hypothesis of a beamed X-ray flux; and (d) the measurements confirm the hypothesis by Cooray et al. (2010) that, although the possibility of accelerating electrons to runaway mode increases with increasing temperature, the lower channel temperature of a defunct channel is compensated by a relatively large leader current.

References

Cooray, V., Dwyer, J. R., Rakov, V., & Rahman, M. (2010). On the mechanism of X-ray production by dart leaders of lightning flashes. *Journal of Atmospheric and Solar-Terrestrial Physics*, *72*(11-12), 848–855. https://doi.org/10.1016/j.jastp.2010.04.006

Dwyer, J. R., Rassoul, H. K., Al-Dayeh, M., Caraway, L., Chrest, A., Wright, B., et al. (2005). X-ray bursts associated with leader steps in cloud to ground lightning. *Geophys. Res. Lett*, *32*(1), L01803. https://doi.org/10.1029/2004GL021782

Dwyer, J. R., Rassoul, H. K., Al-Dayeh, M., Caraway, M., Wright, B., Chrest, A., et al. (2004). Measurements fo X-ray emission from rocket-triggered lightning. *Geophys. Res. Lett*, *31*(5), L05118. https://doi.org/10.1029/2003GL018770

Dwyer, J. R., Schaal, M., Rassoul, H. K., Uman, M. A., Jordan, D. M., & Hill, D. (2011). High-speed X-ray images of triggered lightning dart leaders. *J. Geophys. Res.*, *116*(D20), D20208. https://doi.org/10.1029/2011JD015973

Dwyer, J. R., Uman, M., Rassoul, H. K., Al-Dayeh, M., Caraway, M., Jerauld, J., et al. (2003). Energetic radiation produced during rocket-triggered lightning. *Science*, *299*(5607), 694–697. https://doi.org/10.1126/science.1078940

Hettiarachchi, P., Cooray, V., Diendorfer, G., Pichler, H., Dwyer, J., & Rahman, M. (2018). X-ray observations at Gaisberg Tower. *Atmosphere*, *9*(1), 20. https://doi.org/10.3390/atmos9010020

Howard, J., Uman, M. A., Biagi, C., Hill, D., Jerauld, J., Rakov, V. A., et al. (2010). RF and X-ray source locations during the lightning attachment process. *Journal of Geophysical Research*, *115*(D6). https://doi.org/10.1029/2009JD012055

Kodali, V., Rakov, V. A., Uman, M. A., Rambo, K. J., Schnetzer, G. H., Schoene, J., & Jerauld, J. (2005). Triggered-lightning properties inferred from measured currents and very close electric fields. *Atmospheric Research*, *76*(1-4), 355–376. https://doi.org/10.1016/j.atmosres.2004.11.036

Mallick, S., Rakov, V. A., & Dwyer, J. R. (2012). A study of X-ray emissions from thunderstorms with emphasis on subsequent strokes in natural lightning. *Journal of Geophysical Research*, *117*, D16107. https://doi.org/10.1029/2012JD017555

Montanyà, J., Fabró, F., van der Velde, O. A., Romero, D., Solà, G., Hermoso, J. R., et al. (2014). Registration of X-rays at 2500 m altitude in association with lightning flashes and thunderstorms. *Journal of Geophysical Research*, *119*. https://doi.org/10.1022/2013JD021011

Montanyà, J., O.A. van der Velde, V. March, D. Romero, G. Solà, N. Pineda, (2012), High-speed video of lightning and X-ray pulses during the 2009-2010 observation campaigns in northeastern Spain. *Atmospheric Research*, *117*, D16107. https://doi.org/10.1016/j.atmosres.2011.09.013, 91, 98

Moore, C. B., Eack, K. B., Aulich, G. D., & Rison, W. (2001). Energetic radiation associated with lightning stepped-leaders. *Geophys. Res. Lett.*, *28*(11), 2141–2144. https://doi.org/10.1029/2001GL013140

Naccarato, K. P., & Pinto, O. Jr. (2009). Improvements in the detection efficiency model for the Brazilian lightning detection network (BrasilDAT). *Atmos. Res.*, *91*(2-4), 546–563. https://doi.org/10.1016/j.atmosres.2008.06.019

Saba, M. M. F., Paiva, A. R., Schumann, C., Ferro, M. A. S., Naccarato, K. P., Silva, J. C. O., et al. (2017). Lightning attachment process to common buildings. *Geophys. Res. Lett.*, *44*(9), 4368–4375. https://doi.org/10.1002/2017GL072796

Saleh, Z., Dwyer, J., Howard, J., Uman, M., Bakhtiari, M., Concha, D., et al. (2009). Properties of the X-ray emission from rocket-triggered lightning as measured by the Thunderstorm Energetic Radiation Array (TERA). *Journal of Geophysical Research*, *114*(D17), D17210. https://doi.org/10.1029/2008JD011618

Schaal, M. M., Dwyer, J. R., Arabshahi, S., Cramer, E. S., Lucia, R. J., Liu, N. Y., et al. (2014). The structure of X-ray emissions from triggered lightning leaders measured by a pinhole-type X-ray camera. *J. Geophys. Res. Atmos.*, *119*(2), 982–1002. https://doi.org/10.1002/2013JD020266

Schaal, M. M., Dwyer, J. R., Saleh, Z. H., Rassoul, H. K., Hill, J. D., Jordan, D. M., & Uman, M. A. (2012). Spatial and energy distributions of X-ray emissions from leaders in natural and rocket triggered lightning. *J. Geophys. Res.*, *117*(D15), D15201. https://doi.org/10.1029/2012JD017897

Stolzenburg, M., Marshall, T. C., Karunarathne, S., Karunarathna, N., & Orville, R. E. (2014). Branched dart leaders preceding lightning return strokes. *J. Geophys. Res. Atmos.*, *119*(7), 4228–4252. https://doi.org/10.1002/2013JD021254